FIELD MAP MODEL FOR THE ESS LINAC SIMULATOR

E. Laface* ESS, Lund, Sweden
I. List, Cosylab, Ljubljana, Slovenia

Abstract

The proton beam driving the spallation process at the European Spallation Source, in Lund, will be accelerated and delivered onto a tungsten target by a linac. This linac is composed of four different families of accelerating structures: a drift tube linac, a section of spoke resonators and two sections of elliptical cavities for the particles' medium and high relativistic β. These structures provide 99.8% of the total energy gained by the beam along the accelerator. It is necessary, then, to have an accurate model describing the physics of the cavities in the ESS Linac Simulator (ELS), which is the online model that will simulate the accelerator during operation. Here, we present an RF-cavity model based on the field maps that we implemented in ELS, showing a maximum 10% deviation from TraceWin in the horizontal, vertical and longitudinal planes.

INTRODUCTION

In order to accurately model the accelerating components used in the ESS Proton Linac, the beam physics team is adopting a description of the electromagnetic field based on one-dimensional maps. Each spoke resonator and RF cavity is characterized by a file containing the value of the longitudinal electric field measured along the axis of symmetry (z axis). This field has a sinusoidal behaviour in the inner part of a cavity and an exponential decay on the two ends, as described in [1].

These field maps are then used to calculate the matrix representing the linear part of the equations of motion of a particle subjected to each field. The result is used to transport the beam envelope by applying the matrix of the linear elements to the covariant matrix of the beam.

To calculate the equations of motion we used two different approaches: the first evaluates the contribution of each step of the field map on the variation of the x', y' and z' momenta components for a particle, applying it as thin kicks. With this method, more precise cavity sampling improves accuracy. The second approach is to integrate the field in a certain number of cells (the NCell method), using the Transit Time Factor [2] to evaluate the proper phase and energy changes between cells. Each cell is then treated as a thin accelerating gap in the middle of a drift.

Both methods are then compared with the code used for the design of the ESS Proton Linac—TraceWin [3]—which can simulate the same kind of field maps.

* Emanuele.Laface@esss.se

FIELD MAPS

The transversal normalized momenta can be written in the paraxial approximation as

$$x' = \frac{dx}{ds} = \frac{dx/dt}{ds/dt} \approx \frac{p_x}{p_s} \tag{1}$$

$$y' = \frac{dy}{ds} = \frac{dy/dt}{ds/dt} \approx \frac{p_y}{p_s} \tag{2}$$

we will evaluate x', noting that the same treatment is valid for y'. The variation of momentum in x is given by

$$\begin{aligned} \frac{dx'}{ds} &\approx \frac{d(p_x/p_s)}{ds} = \frac{d(p_x/p_s)}{dt}\frac{dt}{ds} = \frac{\dot{p}_x p_s - p_x \dot{p}_s}{p_s^2}\frac{dt}{ds} \\ &\approx \frac{1}{\beta_s c}\frac{\dot{p}_x - x'\dot{p}_s}{p_s} = \frac{\dot{p}_x - x'\dot{p}_s}{\gamma_s \beta_s^2 mc^2} \end{aligned} \tag{3}$$

where β_s and γ_s are the relativistic parameters of the particle traveling in the s direction and the dot represents the time derivative.

The $\dot{p}_x$ and $\dot{p}_z$ components can be evaluated in terms of the Lorentz force

$$\frac{d\vec{p}}{dt} = q\left(\vec{E} + \frac{\vec{p}}{\gamma m} \times \vec{B}\right) \tag{4}$$

and, again using the paraxial approximation $p_z \approx p_s$, which is valid for the transverse plane, we have

$$\dot{p}_x = q\left(E_x + \frac{p_y B_z - p_z B_y}{\gamma m}\right) \approx q\left(E_x + p_s \frac{y' B_z - B_y}{\gamma m}\right) \tag{5}$$

and

$$\dot{p}_s = q\left(E_z + \frac{p_x B_y - p_y B_x}{\gamma m}\right) \approx q\left(E_z + p_s \frac{x' B_y - y' B_x}{\gamma m}\right) \tag{6}$$

where the quantities $x'B_y$ and $y'B_x$ are always zero because the velocity is parallel to the magnetic field, then

$$\dot{p}_s = qE_z. \tag{7}$$

Substituting Eqs. (5) and (7) into (3) we have

$$\frac{dx'}{ds} = \frac{q}{\gamma_s \beta_s^2 mc^2}\left(E_x + p_s \frac{y' B_z - B_y}{\gamma m} - x' E_z\right). \tag{8}$$

For our model, we are interested in the linear part of the fields where the following equations hold

$$E_x = \frac{\partial E_x}{\partial x} x, \quad E_y = \frac{\partial E_y}{\partial y} y \tag{9}$$

$$E_z = E_{z0}(s)\cos(\omega t + \phi) \tag{10}$$

$$B_x = \frac{\partial B_x}{\partial y} y, \quad B_y = \frac{\partial B_y}{\partial x} x \tag{11}$$

$$B_z = 0 \tag{12}$$

and where ω is the frequency of the cavity and ϕ is the phase. Substituting these equations into Eq. (8), we have

$$\frac{dx'}{ds} = \frac{q}{\gamma_s \beta_s^2 mc^2}\left(\frac{\partial E_x}{\partial x} x - \beta_s c \frac{\partial B_y}{\partial x} x - x' E_z\right). \tag{13}$$

ISBN 978-3-95450-168-7

For the vertical plane y, the calculation is the same and the result is

$$\frac{dy'}{ds} = \frac{q}{\gamma_s \beta_s^2 mc^2}\left(\frac{\partial E_y}{\partial y}y + \beta_s c\frac{\partial B_x}{\partial y}y - y'E_z\right) \quad (14)$$

while for the longitudinal plane we have

$$\frac{dz'}{ds} = \frac{q}{\gamma_s \beta_s^2 mc^2}\left(\frac{1}{\gamma_s^2}\frac{\partial E_z}{\partial z}z - z'E_z\right). \quad (15)$$

The only information provided in the field map is E_z, meaning that E_x, E_y, B_x and B_y are calculated as functions of E_z. This is possible because of the cylindrical symmetry of the cavity and the boundary conditions requiring that the fields vanish at the edge of the cavity. A full treatment of this fact can be found in [1].

Equations (13), (14) and (15) express the instantaneous kick that can be used to evaluate the dynamics for a small space interval ds. The sum of all the kicks along the cavity is essentially an integrator that enumerates the motion of a particle in the electromagnetic field. The validity of these equations is limited to particles close to the central axis because of the linearization of the field.

NCELLS

An alternative method to calculating the beam dynamics of a particle in an RF cavity is to evaluate the Time Transit Factor (TTF) and consequently the equations of motion, as described in [2]. The definition of TTF as function of the relativistic factor β is

$$T(\beta) = \frac{1}{E_0}\int_{-\infty}^{\infty} E_{z0}(s)\cos(\phi(s) - \phi_s)ds \quad (16)$$

where E_0 is the maximum amplitude of the field, $\phi(s) = \frac{2\pi}{\beta\lambda}s$, λ is the wavelength of the RF frequency and ϕ_s is the synchronous phase defined such that

$$\int E_{z0}(s)\sin(\phi(s) - \phi_s)ds = 0. \quad (17)$$

The energy gain for the reference particle is given by

$$\Delta W = q\int_{-\infty}^{\infty} E_{z0}(s)\cos(\phi(s))ds = qE_0T(\beta)\cos(\phi_s). \quad (18)$$

For the transverse horizontal (x) component, we can assign $x = x_0 + zx_0'$, $x' = x_0'$ and $k = \frac{2\pi}{\beta\lambda}$ and integrate Eq. (13)

$$\beta\gamma\Delta x \approx \frac{q}{\beta_s mc^2}\left(\int (x_0 + zx_0')\left(\frac{\partial E_x}{\partial x} - \beta_s c\frac{\partial B_y}{\partial x}\right)ds - x_0'\int E_z ds\right). \quad (19)$$

After some manipulation (assuming the field vanishes at the endpoints) we finally obtain the coefficients

$$k_{11} = 1 - \frac{q}{2\bar{\beta}^2\bar{\gamma}^3 mc^2}\left(\bar{\gamma}^2 + k\frac{T'(\beta)}{T(\beta)}\right)E_0T(\beta)cos(\phi_s) \quad (20)$$

$$k_{22} = 1 - \frac{q}{2\bar{\beta}^2\bar{\gamma}^3 mc^2}\left(\bar{\gamma}^2 - k\frac{T'(\beta)}{T(\beta)}\right)E_0T(\beta)cos(\phi_s) \quad (21)$$

$$k_{21} = -\frac{qkE_0T(\beta)\sin(\phi_s)}{2\bar{\beta}\bar{\gamma}^2 mc^2} \quad (22)$$

where

$$T'(\beta) = \frac{1}{E_0}\int_{-\infty}^{\infty} zE_{z0}(s)\sin(\phi(s) - \phi_s)ds. \quad (23)$$

The $\bar{\gamma}$ denotes the average between γ at the entrance and exit of the cavity and correspondingly for $\bar{\beta}$ and β.

The transport matrix for the single accelerating gap is then

$$G_x = \begin{pmatrix} k_{11}C & 0 \\ \frac{k_{21}}{(\beta\gamma)_f} & k_{22}C \end{pmatrix}. \quad (24)$$

where $(\beta\gamma)_f$ denotes the relativistic factors calculated at the exit of the cavity. The C coefficient is needed because the matrix is obtained as a first order approximation of the real solution, so it is not fully symplectic. That is, C adjusts the determinant such that it is the ratio between the energy at the entrance and the exit of the cavity: $\frac{(\beta\gamma)_i}{(\beta\gamma)_f}$. The matrix for the vertical plane G_y is identical to G_x.

For the longitudinal z plane, the substitution is $z = z_0 + \frac{1}{\gamma^2}z\delta_0$, $\delta = \delta_0$. Integrating Eq. (15), we obtain the coefficients

$$k_{21} = \frac{qkE_0T(\beta)\sin(\phi_s)}{\bar{\beta}^2 mc^2} \quad (25)$$

$$G_z = \begin{pmatrix} \frac{\gamma_f}{\gamma_i} & 0 \\ \frac{k_{21}}{\gamma_i(\beta\gamma^2)_f} & \frac{(\beta\gamma^2)_i}{(\beta\gamma^2)_f} \end{pmatrix}. \quad (26)$$

The matrices calculated here are for one accelerating gap. A cavity is split where the field crosses zero and is represented by several cells. Each cell is simulated by a gap (located at $\frac{\beta\phi_s}{k}$) interleaved with drifts.

RESULTS

The models of NCells and field maps described in the previous sections were implemented in the online simulator ELS, which is contained in the OpenXAL framework [4]. The simulations were performed using the conditions listed in Table 1.

Table 1: Beam Parameters

Parameter	Value
Initial Kinetic Energy	3.62 MeV
Beam Peak Current	62.5 mA
Particles per bunch	1.1×10^9
Duty Cycle	4%
Freq. before the Medium β sect.	352.21 MHz
Freq. after the Medium β sect.	704.42 MHz
Horizontal Normalized Emit.	0.25×10^{-6} m rad
Vertical Normalized Emit.	0.25×10^{-6} m rad
Longitudinal Normalized Emit.	0.36×10^{-6} m rad

The initial energy, 3.62 MeV, occurs at the entrance of the MEBT section. The beam is transported through the DTL, which we represent with 177 RF gaps, then it crosses 26 Spoke resonators, 36 medium-β cavities and finally 84 high-β cavities. The space-charge effects are incorporated as described in [5].

ISBN 978-3-95450-168-7

We can then compare TraceWin operating with the field maps versus ELS operating with NCells or field maps. The first comparison is for the energy gain along the linac. Here, the two models implemented in ELS are in perfect agreement with TraceWin, as shown in Fig. 1, with a relative average difference of 0.15% for the NCells and 0.13% for the field maps.

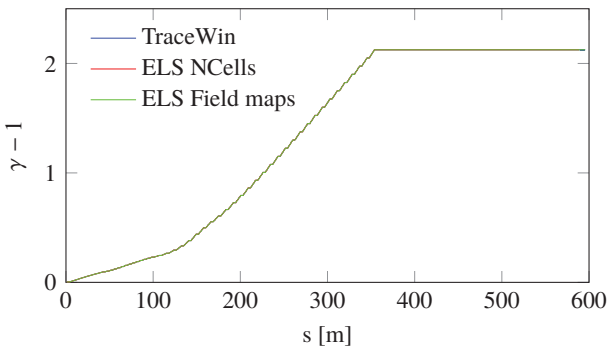

Figure 1: [Color] Energy of the beam expressed in $\gamma - 1$ along the accelerator calculated with the TraceWin field maps, the ELS NCells and the ELS field maps. The three models are in excellent agreement.

The next benchmarks are the three r.m.s. of the beam for the horizontal, vertical and longitudinal planes, shown in Fig. 2: I, II and III, respectively. For the horizontal plane, the values for relative average difference between TraceWin and ELS are 4.58% and 4.56%, respectively, for the NCells and field maps.

For the vertical plane, the values for relative average difference between TraceWin and ELS are 4.35% and 3.88%, respectively, for the NCells and field maps.

The maximum differences between the two ELS models and TraceWin are within 10% in the longitudinal plane.

CONCLUSIONS

We presented here the two methods, numerical field map integrator and NCells, used at ESS to handle the field map description of RF cavities. Both methods are implemented in the ESS Linac Simulator as part of the OpenXAL framework. The comparison with the software TraceWin shows a very good agreement, within 10% of deviation.

REFERENCES

[1] T. Lindqvist and E. Laface, "Field parametrisation for the ESS superconducting cavities," *Proceedings of IPAC 2014, Dresden, Germany*, Jun 2014.

[2] T. P. Wangler, *RF Linear Accelerators, 2nd, Completely Revised and Enlarged Edition*, ser. Physics textbook. Weinheim: Wiley-VCH, Jan 2008.

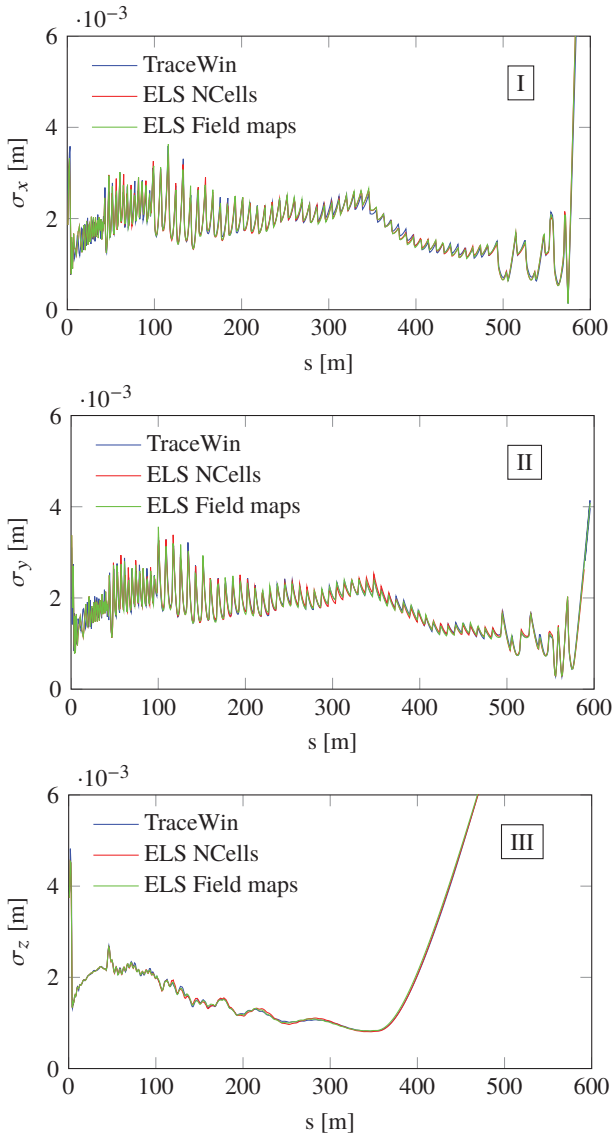

Figure 2: [Color] Standard deviation on the horizontal (I), vertical (II) and longitudinal (III) planes evaluated with the TraceWin field maps, the ELS NCells and the ELS field maps. The three models are in good agreement.

[3] D. Uriot. TraceWin: http://irfu.cea.fr/Sacm/logiciels/index3.php.

[4] T. Pelaia II *et al.*, "Open XAL Status Report 2015," *This conference - MOPWI050*, 2015.

[5] E. Laface *et al.*, "Space Charge and Cavity Modeling for the ESS Linac Simulator," *Proceedings of IPAC 2013, Shanghai, China*, May 2013.